

Photo-induced writing and erasing of gratings in As_2S_3 chalcogenide microresonators

JIANGANG ZHU,¹ THOMAS M. HORNING,² MO ZOHRABI,¹ WOUNJHANG PARK,¹ AND JULIET T. GOPINATH^{1,2,*} 

¹Department of Electrical, Computer and Energy Engineering, University of Colorado Boulder, 425 UCB, Boulder, Colorado 80309, USA

²Department of Physics, University of Colorado Boulder, 425 UCB, Boulder, Colorado 80309, USA

*Corresponding author: juliet.gopinath@colorado.edu

Received 11 August 2020; revised 15 October 2020; accepted 15 October 2020 (Doc. ID 405136); published 18 November 2020

Reconfigurable optical devices provide new opportunities for integrated photonics. The use of chalcogenide glasses, with large refractive index nonlinearity and photosensitivity, in conjunction with the microresonator platform has proven to be a powerful tool in the study and application of nanophotonics. Here, we report cavity-enhanced photo-induced writing and erasing of gratings in a chalcogenide As_2S_3 microresonator. Grating writing is implemented with self-enhanced standing wave modes, while the erasing of written gratings as well as removing of intrinsic back-scattering is achieved by Kerr-nonlinearity-induced symmetry breaking in the microresonator. These findings pave the way for future reconfigurable photonic devices and reveal exciting new possibilities for nonlinear photonics and microresonators. © 2020 Optical Society of America under the terms of the [OSA Open Access Publishing Agreement](https://doi.org/10.1364/OPTICA.405136)

<https://doi.org/10.1364/OPTICA.405136>

Chalcogenide glasses are attractive optical materials due to their large linear and nonlinear refractive indices, wide transmission window from near- to far-infrared, and low phonon energy [1,2]. They have generated great interest for nonlinear optical devices, with applications in sensing and communications [3]. Photosensitivity is a well-known property of these glasses, in which chemical bonds change when exposed to light with a wavelength above or, in some cases, slightly below the bandgap [4,5]. This includes observation of phenomena such as photodarkening, photodiffusion, photofluidity, photocrystallization, and photo-induced birefringence [6]. In chalcogenide devices, two causes are considered: (1) photo-induced refractive index change and (2) photo-densification or expansion [7]. While the phenomenon can be viewed negatively, in this work, we show that photosensitivity can be exploited, for the first time, to generate reconfigurable optical devices using microresonators with low power.

Photosensitivity has been explored to directly write optical waveguides and waveguide Bragg gratings [8,9]. In chalcogenide microresonator devices, photosensitivity was used to trim the resonance frequency of microresonators and achieve a global shift of resonance modes [10]. In another demonstration, a partially

photo-induced reversible resonance shift was realized by combining photo-expansion and photo-induced index change in a chalcogenide microresonator [7]. Recently, Shen *et al.* reported resonance-mode-specific writing of gratings in chalcogenide microrings [11]. The written gratings can be reconfigured by first erasure with flood illumination of visible light and subsequent rewriting. This is significant progress towards reconfigurable chalcogenide devices. However, a true mode-specific reversible photo-induced application has not been demonstrated in chalcogenide microresonators. The ability to fully reverse the photo-induced changes will be a game changer and enable new reconfigurable photonic devices.

Chalcogenide As_2S_3 microspheres exhibit very high quality-factors ($Q > 10^7$) and photosensitivity at 1550 nm [9,11]. Here, we report the experimental observation of resonant cavity-enhanced, photo-induced writing and erasing of gratings in a high- Q chalcogenide microresonator. Reflective gratings, corresponding to a specific resonance mode, can be written by forming standing wave modes (SWMs) in the resonator. In addition, with higher laser pump power, we demonstrate strong symmetry breaking phenomena in which the resonator allows only a traveling wave mode in one direction, and the propagating mode in the opposite direction is shifted off resonance [12]. This symmetry breaking regime allows mode-specific erasure of written gratings. Compared with Shen's work [11], we made improvements by demonstrating resonance mode-specific removing of gratings in using Kerr symmetry breaking, faster writing and erasing speeds, and a lower optical power requirement. Additionally, for the first time, intrinsic back-scattering in the microresonator, caused by scatterers within the device, can be eliminated. These findings are significant and will enable a slew of new applications for microresonators.

High-quality As_2S_3 microspheres [Fig. 1 inset] are fabricated by melting the end of an As_2S_3 fiber taper [13]. A single-frequency tunable laser at 1550 nm (Toptica CTL 1550) is efficiently coupled to the As_2S_3 microsphere with a silica fiber taper [14]. A fiber circulator is placed at the input side to extract the reflection (P_{CW}). In these microsphere resonators, clockwise (CW) and counter-clockwise (CCW) modes naturally exist. Using a recently developed technique [14], we characterized the As_2S_3 microspheres to determine their intrinsic Q factors, nonlinear index (n_2), and back-coupling rate (g) between CW and CCW

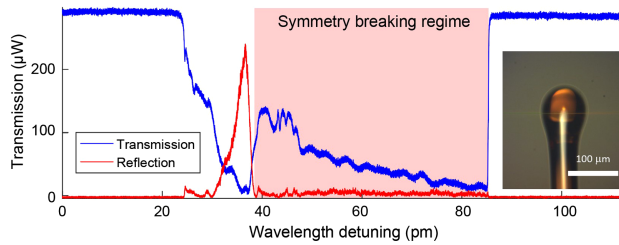


Fig. 1. Nonlinear symmetry breaking in an As_2S_3 microsphere. Transmission (blue) and reflection (red) spectrum during laser wavelength up-scan showing symmetry breaking. Inset shows an image of an As_2S_3 microsphere.

modes. These microspheres have high Q factors of $\sim 10^7$ and n_2 of $\sim 3 \times 10^{-18} \text{ W/m}^2$ [14]. Due to material defects and surface contamination, the back-coupling rate is usually between 500 kHz and 50 MHz. In the case of a large back-coupling rate ($g >$ resonance linewidth), mode splitting can be observed.

The high quality factor of the microresonator and the high nonlinearity allow Kerr-induced symmetry breaking. This phenomenon occurs when a directional traveling wave mode (e.g., CW) is shifted off resonance due to strong cross-phase modulation from the counter-propagating mode (e.g., CCW) [12,15]. In our experiment, we monitor both transmission (CCW mode) and reflection (CW mode). The reflection is due to strong coupling of CW and CCW modes (quantified by g), induced by intrinsic defects and scattering [16]. When the input laser wavelength is tuned closer to the cavity resonance, the reflected mode quickly diminishes, as the CW mode is shifted off resonance due to cross-phase modulation by the CCW mode in the resonator. The Kerr symmetry breaking in an As_2S_3 microsphere was observed at only 300 μW input power, due to the high Q and n_2 of the As_2S_3 microresonator (Fig. 1).

The amplitude of the transmission increases when the system transitions from the strong coupling regime to the symmetry breaking regime. This occurs due to the decrease in coupling between the CW and CCW modes in the symmetry breaking regime. In addition, the resulting thermal red shift of resonance wavelength of CCW mode contributes (detuning between pump and resonance increases). The result is that in the symmetry breaking regime, the CW mode and reflection are eliminated, and only the CCW mode exists in the resonator.

We choose three nearby resonance modes [Fig. 2] to demonstrate writing and erasing of gratings. Figure 2 shows the low power ($< 5 \mu\text{W}$) transmission [(a) and (b)] and reflection spectrum [(a) and (c)] of these three modes. In each of these modes, due to intrinsic defect scattering in the microsphere, there exists a slight initial mode splitting and back-reflection. The mode splitting is induced by scatterers in the resonator that cause the modes (CW and CCW) to couple to the scatterers and each other. The degeneracy between the two SWMs (CW + CCW and CW − CCW) is lifted due to their different spatial distributions, which result in mode splitting [17,18]. Note that in Figs. 2–4, the transmission and reflection are recorded at slightly different times (tens of seconds apart). Thus, there is some small variation in mode locations due to cavity temperature fluctuations and piezo scanning noise.

To write a grating to a specific resonance mode, we scan the pump laser wavelength repeatedly at 25 Hz across a resonance mode. By finely tuning the piezo scanning range of the tunable laser, we limit the laser wavelength range to tens of picometers

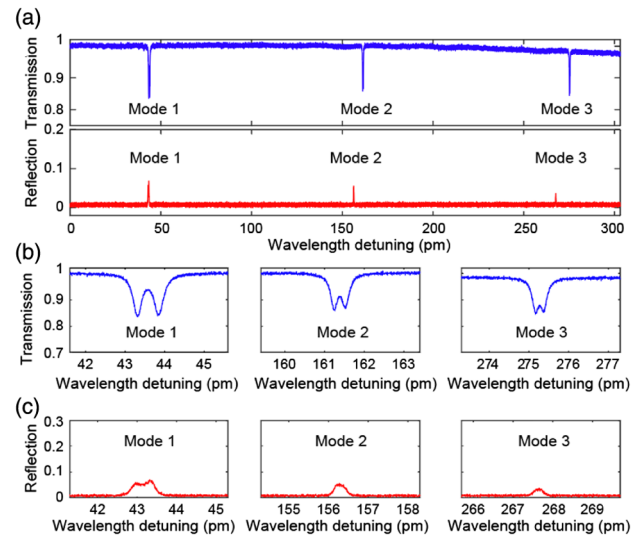


Fig. 2. (a) Transmission (blue) and reflection (red) spectra of three nearby resonance modes. (b), (c) Detailed view of the three modes.

around the mode of interest, without exciting the nearby modes. We excite the resonance mode by pumping in the CCW direction. Due to the intrinsic scattering and resulting back-coupling, both CW and CCW modes are excited. The superposition of the CW and CCW modes gives rise to a set of SWMs. A grating pattern similar to a microgear resonator [19,20] is then written in the resonator by the material photosensitivity with the same periodicity as the SWMs created in the microsphere. This is similar to writing a Bragg grating in a waveguide [21]. For a given mode, the strength of the grating (magnitude of splitting) increases with intra-cavity exposure dosage. We estimate the on-resonance duty cycle of our writing procedure to be about 30%. With input power of $\sim 50 \mu\text{W}$, the splitting amount reaches 90% of maximal in about 10–30 s in our experiments. Due to the orthogonality of different resonance modes, the grating is mode specific. A grating corresponding to a particular mode does not affect other modes.

Removing or erasing a grating requires the Kerr symmetry breaking regime, and can be accessed by increasing the pump power compared to grating writing. In our case, the threshold for this regime is 300 μW . Symmetry breaking enables a strong forward circulating mode (CCW) and the absence of a backward circulating mode (CW). This special condition, coupled with photosensitivity, effectively removes any grating structure, reflection, or mode splitting from the resonance mode. Significantly, it also compensates for the defect-induced back-scattering and coupling in the microsphere and erases the resulted mode splitting and reflection. The mechanism is likely due to the photo-induced compensation (index or photo-expansion/densification) of any local variation in the microsphere by the strong single-direction circulating light. This process takes tens of seconds with an input power level of 300 μW . After erasing, the mode reflection and mode splitting drop to very low levels and cannot be observed in the transmission and reflection spectra.

We use five steps to demonstrate the writing and erasing of mode-specific gratings. In each step, an input pump power is used to perform grating writing ($\sim 50 \mu\text{W}$) or erasing ($\sim 300 \mu\text{W}$) on an individual mode. Very low powers ($< 5 \mu\text{W}$) are used to examine the transmission and reflection spectra of the three modes. In Figs. 3 and 4, we show the low power transmission and reflection

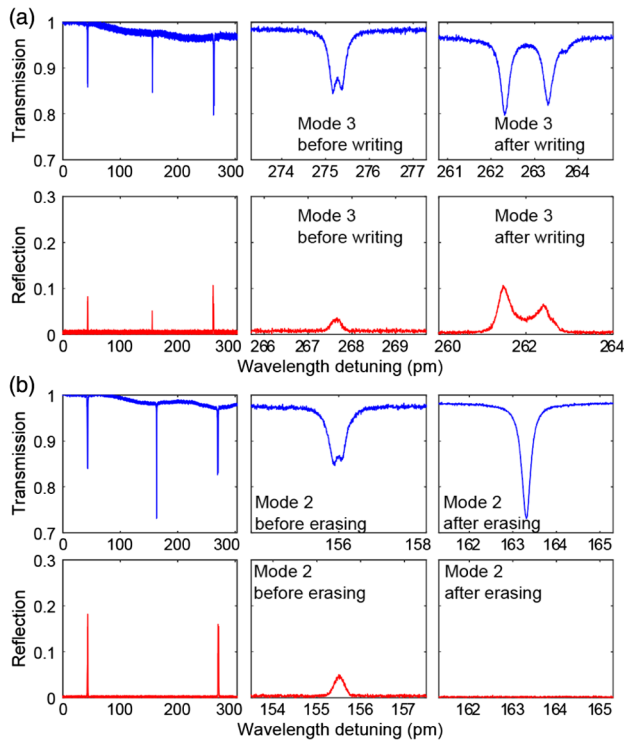


Fig. 3. Photosensitive writing and erasing of selective modes. (a) Left column: transmission (blue) and reflection (red) spectra of three modes after writing to mode 3. Middle column: mode 3 before writing. Right column: mode 3 after writing. (b) Left column: transmission (blue) and reflection (red) spectra after erasing mode 2. Middle column: mode 2 before erasing. Right column: mode 2 after erasing.

spectra after each writing or erasing operation. To write a grating, we write to mode 3 (defined in Fig. 2) with 50 μW of laser power. The on-resonance pumping creates SWMs and induces photosensitive changes in the As_2S_3 microsphere. With SWMs, the strength of the photo-induced grating increases over time (tens of seconds), and the back-coupling and SWMs are further enhanced. After the grating strength slowly saturates in tens of seconds, we take measurements at low optical input power.

Figure 3(a), left column, shows the spectrum of the three modes again after writing a grating to mode 3, in both transmission and reflection. Modes 1 and 2 are unaffected. The middle column shows the zoomed-in transmission and reflection on mode 3 before writing, in which some mode splitting is observed. The right-hand column shows the transmission and reflection of mode 3, after writing. Strong mode splitting and reflection on mode 3 are observed in the low power spectra. Because modes 1 and 2 are not affected, this indicates the changes in mode 3 are the result of a grating-like structure. If it is a change of a local site, modes 1 and 2 should also show significant changes in mode splitting and reflection amplitude, which is not the case. Due to the spatial orthogonality of different modes, a grating-like variation corresponding to one mode does not affect the modal coupling of another mode. In the second step, we pump mode 2 with 300 μW of power over tens of seconds to erase the mode, by exciting the symmetry breaking condition. This operation is illustrated in Fig. 3(b). The left-hand column shows the spectra of the three modes after erasing mode 2. The middle column shows the zoomed-in transmission and reflection spectra of mode 2 before erasing, and the right-hand column, after erasing. The erasing

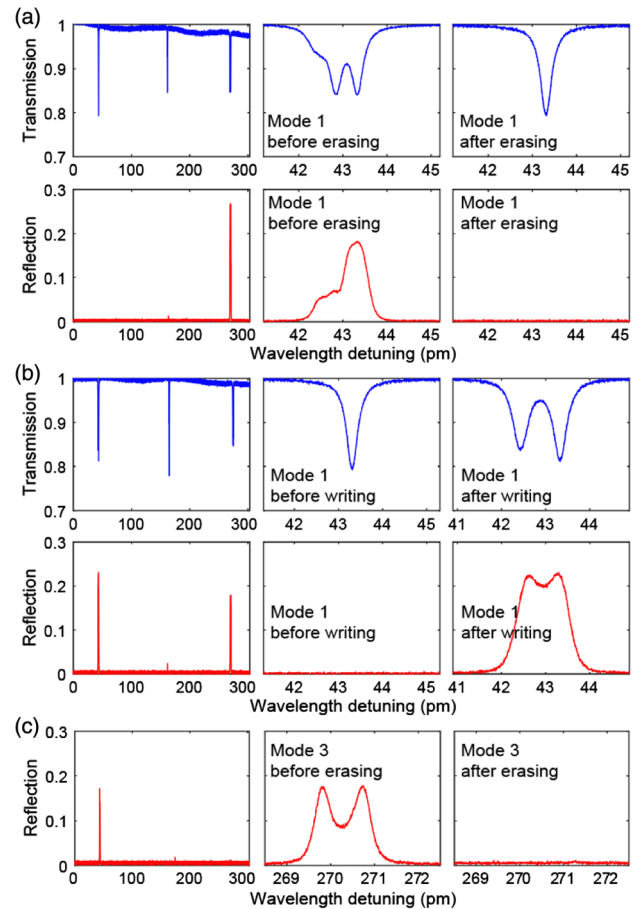


Fig. 4. Photosensitive writing and erasing of selective modes. (a) Left column: transmission (blue) and reflection (red) spectra of three modes after erasing mode 1. Middle column: mode 1 before erasing. Right column: mode 1 after erasing. (b) Left column: transmission (blue) and reflection (red) spectra of three modes after writing to mode 1. Middle column: mode 1 before writing. Right column: mode 1 after writing. (c) Left column: reflection spectra of three modes after erasing mode 3. Middle column: mode 3 before erasing. Right column: mode 3 after erasing.

operation removes the reflection completely and restores complete transmission. Only the forward circulating mode (CCW) is allowed (grating erasing). The data show that the erasing operation can remove or compensate for any intrinsic scattering or back-coupling affecting mode 2. However, modes 1 and 3 are not significantly affected in terms of splitting and reflection, evident by their almost unchanged resonance lineshapes. The increased coupling depth of mode 2 after the erasing operation is due to the recombining of the mode power in previous split modes (degenerate to non-degenerate). This proves that the erasing operation is also mode specific.

In the third step, we erase reflection/back-coupling on mode 1 [Fig. 4(a)]. The left-hand column shows the three mode spectra after erasing mode 1. The middle column shows the transmission and reflection spectra of mode 1 before erasing. The right column shows the transmission and reflection spectra of mode 1 after erasing. Mode 1 shows a single transmission resonance dip and no reflection. Next, we write a grating on mode 1, causing it to split and produce strong reflection, while modes 2 and 3 are unchanged. In Fig. 4(b), the left-hand column shows the three-mode spectra

after writing a grating to mode 1. The middle column shows the transmission and reflection spectra of mode 1 before writing. The right column shows the transmission and reflection spectra of mode 1 after writing the grating. This result shows that grating writing can start from an already erased mode. The necessary seeding of initial SWMs to start grating writing can be from physical perturbations of the microcavity (nanoparticles in air, temperature fluctuation, etc.) and reflection of downstream fiber optics. In the final step, to demonstrate that we can remove a written grating, we erase the grating/reflection on mode 3. In Fig. 4(c), the left-hand column shows the three-mode reflection spectra after erasing the grating written to mode 3. The middle column shows the reflection spectrum of mode 3 before the operation. The right column shows the reflection spectrum of mode 3 after erasing the written grating. Note that in Figs. 3 and 4, the amplitude of modes should be viewed qualitatively, as fiber coupling requires manual adjustment during the experiment time of about 1 h, and thus the coupling is not constant. The slight wavelength misalignment of modes in these figures is due to laser and resonator wavelength drift, piezo scan noise, and the resulting wavelength detuning difference.

The photo-induced writing and erasing steps in the previous section prove these operations are repeatable and mode specific. The selectivity should hold for all modes except for the rare cases of two modes having overlapped and phased matched spatial distributions, which is yet to be observed in experiments. At the power levels used, it takes tens of seconds to write or erase a mode by scanning laser repeatedly across it, which may not be fast enough for some applications. To reduce the grating writing time and increase grating strength, one could use a laser wavelength closer to the band edge, as well as using different materials with stronger photo-sensitivity and locking the laser wavelength to the resonance. We also observed grating writing at a low power level $<5 \mu\text{W}$, but at a much slower rate. We did not observe a threshold power for grating writing. Thus, we think the overall on-resonance exposure dosage (per optical volume/area) is the determining factor for grating strength. In principle, if a broadband light source can be efficiently coupled to the resonance modes, it should also enable grating writing due to the wavelength selectivity of high- Q resonances. In our experiments, we did not see a significant shift in resonance modes larger than resonance thermal drift, indicating the global mode index or resonator size is unchanged. This is significantly different from previous work [7,11]. The written gratings last as long as the As_2S_3 microsphere in room conditions (for about four weeks before degradation in the cavity Q factor).

It is critical to control the power in the nonlinear regime, as increasing power above 1 mW causes Q degradation of the high- Q As_2S_3 microspheres with diameters around 100 μm . Too much power could induce excessive heat and material refractive change through annealing. If multiple nearby modes have similar coupling conditions and polarization, it is possible to erase them in one operation by scanning the laser repeatedly across them. Erasing also induces distributed local variations to compensate for intrinsic defects- (such as dust particles) induced scattering in a specific mode. The resonance mode is “cleaned” after the erasing operation and free of any observable mode splitting and reflection. This discovery is significant, as it provides a unique way to modify and engineer microresonators. For example, external scattering centers (such as fiber tip probes) can be introduced to the mode volume of a microresonator, and after the erasing operation with the scattering centers in the mode volume, all scattering/back-coupling will be removed/compensated for. Then, if the external scattering centers

are removed, the microresonator will have the properties of the scattering centers as if the external perturbation is still in the mode volume. Using this technique, an arbitrary “mask” can be used to imprint a designed pattern to a microresonator. The exact mechanism of erasing and photo-induced engineering of microresonators will be investigated in depth in future work.

In summary, we observed symmetry breaking and photo-induced writing and erasing of gratings on individual resonance modes in an As_2S_3 microsphere. The gratings written to each mode can coexist, due to their orthogonal spatial distributions. The achieved high selectivity on resonance mode, and full extinction of reflection mode could enable high-performance reconfigurable photonic reflectors/filters. The method of erasing back-reflection of a resonance mode can allow imprinting arbitrary scattering patterns to a mode. These findings and techniques could extend to other photosensitive microresonator devices and pave the way towards future photonic circuits.

Funding. University of Colorado Boulder; Office of Naval Research (N00014-19-1-2251); Air Force Office of Scientific Research (FA9550-15-1-0506, FA9550-19-1-0364); Defense Advanced Research Projects Agency (W911NF-15-1-0621).

Acknowledgment. We are grateful to Michael Grayson for technical discussions.

Disclosures. The authors declare no conflicts of interest.

REFERENCES

1. A. Zakery and S. R. Elliott, *J. Non-Crystalline Solids* **330**, 1 (2003).
2. M. Grayson, M. Zohrabi, K. Bae, J. Zhu, J. T. Gopinath, and W. Park, *Opt. Express* **27**, 33606 (2019).
3. B. J. Eggleton, *Opt. Express* **18**, 26632 (2010).
4. K. Shimakawa, A. Kolobov, and S. R. Elliott, *Adv. Phys.* **44**, 475 (1995).
5. H. Fritzsche, *Insulating and Semiconducting Glasses* (World Scientific, 2000), Vol. **17**, p. 653.
6. B. J. Eggleton, B. Luther-Davies, and K. Richardson, *Nat. Photonics* **5**, 141 (2011).
7. N. Singh, D. D. Hudson, R. Wang, E. C. Mägi, D.-Y. Choi, C. Grillet, B. Luther-Davies, S. Madden, and B. J. Eggleton, *Opt. Express* **23**, 8681 (2015).
8. H. Ebendorff-Heidepriem, *Opt. Mater.* **25**, 109 (2004).
9. R. Ahmad and M. Rochette, *Appl. Phys. Lett.* **99**, 061109 (2011).
10. J. Hu, M. Torregiani, F. Morichetti, N. Carlie, A. Agarwal, K. Richardson, L. C. Kimerling, and A. Melloni, *Opt. Lett.* **35**, 874 (2010).
11. B. Shen, H. Lin, S. S. Azadeh, J. Nojic, M. Kang, F. Merget, K. A. Richardson, J. Hu, and J. Witzens, *ACS Photon.* **7**, 499 (2020).
12. L. Del Bino, J. M. Silver, S. L. Stebbings, and P. Del’Haye, *Sci. Rep.* **7**, 43142 (2017).
13. F. Vanier, P. Bianucci, N. Godbout, M. Rochette, and Y. Peter, *International Conference on Optical MEMS & Nanophotonics* (2012), pp. 45–46.
14. J. Zhu, M. Zohrabi, K. Bae, T. M. Horning, M. B. Grayson, W. Park, and J. T. Gopinath, *Optica* **6**, 716 (2019).
15. A. E. Kaplan and P. Meystre, *Opt. Lett.* **6**, 590 (1981).
16. A. Mazzei, S. Götzinger, L. de S. Menezes, G. Zumofen, O. Benson, and V. Sandoghdar, *Phys. Rev. Lett.* **99**, 173603 (2007).
17. J. Zhu, S. K. Ozdemir, Y.-F. Xiao, L. Li, L. He, D.-R. Chen, and L. Yang, *Nat. Photonics* **4**, 46 (2010).
18. M. L. Gorodetsky, A. D. Pryamikov, and V. S. Ilchenko, *J. Opt. Soc. Am. B* **17**, 1051 (2000).
19. K. P. Huy, A. Morand, and P. Benech, *IEEE J. Quantum Electron.* **41**, 357 (2005).
20. V. M. N. Passaro, F. De Leonardis, and G. Z. Mashanovich, *Opt. Express* **15**, 797 (2007).
21. K. O. Hill and G. Meltz, *J. Lightwave Technol.* **15**, 1263 (1997).